

Development of Polypropylene Nanocomposites Filled with Clay Particles from Cubati/Brazil

Carlos I. R. de Oliveira¹, Marisa C. G. Rocha^{1,*}, Joaquim T. de Assis¹,
Nancy I. Alvarez Acevedo¹, Ana L. N. da Silva², Luiz C. Bertolino³

¹Instituto Politécnico- IPRJ, Universidade do Estado do Rio de Janeiro - UERJ, Nova Friburgo, Brazil

²Instituto de Macromoléculas Professora Eloisa Mano - IMA, Universidade Federal do Rio de Janeiro – UFRJ, Rio de Janeiro, Brazil

³Centro de Tecnologia Mineral - CETEM, Ministério da Ciência, Tecnologia e Inovações - MCTI, Rio de Janeiro, Brazil

Abstract The aim of this work is to expand the field of applications of bentonite clays from Cubati, Paraíba, through the development of polymeric nanocomposites. A Brazilian bentonite clay from Cubati, Paraíba, was used to produce an organophilic clay. The pristine and modified clays were characterized by infrared spectroscopy (FTIR), X-ray fluorescence (XRF) and X-ray diffraction (XRD). The results indicated that the clay was organophilized. The PP/clay nanocomposites were prepared with 3 wt% of organoclay and 5 wt% of a polypropylene grafted maleic anhydride (PP-g-MA) in a co-rotating twin-screw extruder. The produced materials were characterized by XRD, transmission electron microscopy (TEM), differential scanning calorimetry (DSC) and thermogravimetric analysis (TGA). The tensile properties and impact strength were also determined. The results indicated that PP/PPMA/clay nanocomposite presents higher thermal stability and crystallization temperature than the PP matrix. The PP's Young's modulus and tensile strength were not significantly affected. However, there was a significant increase of the elongation at break. These findings show that Brazilian bentonite clay can be used as a filler in PP nanocomposites.

Keywords Compatibilizer, Characterization, Nanocomposites, Organophilic bentonite, Polypropylene

1. Introduction

Polymer/layered silicate (clay) nanocomposites have been widely studied due to the many advantages these materials present compared to conventional composites [1,2]. The polymer/clay nanocomposites comprise a class of materials in which the inorganic phase is dispersed in the polymer matrix at nanometer level. The main difference between nanocomposites and traditional composites is that processing of nanocomposites requires low filler contents (up to 5% by weight), while traditional composites need high content of filler, up to 40 wt% [3]. Nanocomposites began to be studied in the 1980s by the Toyota Research Laboratory, with the development of nanocomposites of polyamide and clay [4]. Polymer/clay nanocomposites have superior mechanical and thermal properties, flame retardancy and dimensional stability and lower permeability to gases than those presented by the conventional composites [5-7]. Because of this, there are numerous studies on these

materials [8-10].

Among the different clays currently used for the preparation of polymeric nanocomposites, the bentonite clays have long been used, mainly because of their attractive properties, such as very high aspect ratio and surface area. Besides that, these materials are environmentally friendly and available in large quantities. In Brazil, there are large deposits of clays [3,11,12]. Bentonite rocks are composed essentially of one or more minerals (mainly montmorillonite) of the smectite clay group, and the physical properties of the clays are mainly established by this mineral [13,14]. Bentonite is an aluminosilicate 2:1, [(Mg,Ca)O.Al₂O₃Si₅O₁₀.nH₂O)], formed from the decomposition of volcanic ash, which in its natural form has the exchangeable cations Na⁺, Mg²⁺, Ca²⁺, Al³⁺ and Fe³⁺. In Brazil, the most common form of this occurrence is as a polycationic bentonite [11]. Bentonites are very fine-grained clays, with high adsorption capacity, high content of colloidal matter and high possibility of activation. Most Brazilian bentonite reserves, about 62%, are located in the state of Paraíba, in the municipalities of Boa Vista and Cubati. The state of São Paulo accounts for 28% of the reserves and the states of Bahia, Minas Gerais and Paraná account for the remaining 10% [3]. Although, there are many

* Corresponding author:

mrocha@iprj.uerj.br (Marisa C. G. Rocha)

Received: July 2, 2020; Accepted: July 27, 2020; Published: August 15, 2020

Published online at <http://journal.sapub.org/materials>

published studies on clays from Boa Vista, there are few studies on nanocomposite production from Cubati clays [15]. The industrial application of clays requires a complete identification of its nature and properties. Depending on the deposit from which the clay was extracted, there are may be some difference in properties, even for a given clay variety [16]. The reserves in Boa Vista are depleted, it is urgent to assess clays with potential from other deposits in Paraiba, such as Cubati.

Despite the numerous advantages of using bentonite clays to prepare polymer nanocomposites, the natural hydrophilicity of these silicates hinders the interaction and the ability to blend them with non-polar polymeric matrices [8,17]. To improve interaction with the polymer, the clay must be organically modified, giving rise to an organoclay. Among the different processes used to obtain organophilic bentonite clays, the use of quaternary ammonium salts containing chains of different structures is one of the most widely used methods [17]. The presence of organic cations between bentonite clay layers decreases the surface tension of these clays and improves the compatibility with polymeric matrices [18]. The bentonite clays are the most used in the preparation of organophilic clays due to the small size of the crystals, the high cation exchange capacity (CEC), large surface area and good swelling capacity in water [19]. This set of properties allows the rapid intercalation of organic compounds and a reaction yield of 100% [20,21].

Polypropylene (PP) is one of the most widely used non-polar polymers due to its low cost, low density and the high specific properties. In recent years, PP/clay nanocomposites have attracted strong research interest [22-24]. However, the absence of polarity of the PP hinders interaction and intercalation or exfoliation of the polymeric chains between the platelets of the clay particles [25]. Consequently, the matrix modification with polar moieties is necessary prior to modified clay introduction in order to achieve nanometric dispersion of the clay [26]. Several studies have been performed to evaluate the use of polypropylene grafted with maleic anhydride and acrylic acid as compatibilizers in polypropylene/organoclay nanocomposites [26,27].

According to López-Quintanilla *et al.* (2006) in the melt process of obtaining nanocomposites, the exfoliation and dispersion of nanoclays in polypropylene is a function of some parameters such as: type of clay and its pretreatment method, concentration of functional groups in the compatibilizer and its overall concentration in the composite, the viscosity of the polymer, and the operational conditions [26].

The aim of this work is to expand the field of applications of bentonite clays from Cubati through the development of polymeric nanocomposites. For this purpose, in this work, polypropylene/clay nanocomposites were prepared and their properties were determined. The efficiency of polypropylene grafted with maleic anhydride (PP-g-MA) as a compatibilizing agent was also evaluated.

2. Experimental

2.1. Materials

Polypropylene homopolymer (PP, H501HC) with a melt flow index (MFI) of 3.5 g/10 min (230°C/2.16 kg), supplied by Braskem S.A., was used. Polypropylene grafted with maleic anhydride (PP-g-MA), Polybond 3200, with a melt flow index (MFI) of 109 g/10 min (190°C/2,16 Kg) and having 2.7 wt% MA content was supplied by Chemtura Indústria Química do Brasil Ltda. Bentonite clay from Cubati, Paraíba, a municipality located in the northeastern region of Brazil (geographical coordinates 24M 0799950 9245922), was used. The clay sample was sifted by passing it through ABNT 635 mesh (0.022 mm) and identified according to its source as JG clay. The quaternary ammonium salt, cetyltrimethyl ammonium chloride, commercially known as Dehyquart® A, from Famos Química Fina, was used to modify the bentonite.

2.2. Preparation of Organoclay

To make the interlayer spacing more homogeneous and regular, the JG clay was treated with a solution of sodium chloride. In this treatment, 100 g of JG clay, 500 g of NaCl and 1000 ml of deionized water were placed in a glass reactor equipped with a mechanical stirrer. The system was heated in a water bath at 55°C and kept under stirring for 72 hours. Subsequently, the product was centrifuged with deionized water (2000 ml) for 45 minutes at 2000 rpm to remove the Cl⁻ anions. The absence of Cl⁻ anions was confirmed by titration with 0.1 M AgNO₃. Then the homoionic clay was dried at 60°C for 48 h in an oven with air circulation, ground and screened with a 200 mesh sieve.

To obtain the organophilic clay using the quaternary ammonium salt (cetyltrimethyl ammonium chloride, a dispersion containing 60 g of sodium clay, 72 g of quaternary ammonium salt and 1200 ml of deionized water was prepared in a glass reactor equipped with a mechanical stirrer. The system was heated in a water bath at 55°C and kept under stirring for 72 hours. Subsequently, the product was centrifuged with deionized water (2000 ml) for 45 minutes at 2000 rpm to remove the Cl⁻ anions. The absence of Cl⁻ anions was confirmed by titration with 0.1 M AgNO₃. The organophilic clay was dried at 60°C for 48 h in an oven with air circulation, ground and screened with a 200 mesh sieve and stored for further characterization.

2.3. Preparation of Nanocomposites

Prior to blending, PP and organoclay were oven dried at 60°C for 24 h. The PP-g-MA was placed in a desiccator for 24 h before blending. These components were physically mixed and then extruded in a Teck Tril model DCT 20 co-rotating twin-screw extruder (L/D ratio of 36). The extrusion was performed with a temperature profile equal to 90/120/160/180/180/190/190/200/200/210°C (from the feed to the die zone). The screw speed was set at 500 rpm. The nanocomposites were prepared by dispersing the

modified bentonite (3 wt%) into the polypropylene matrix without and with 5 wt% of PP-g-MA. The pellets obtained were injection molded in an Arburg model Allrounder 270 S molding machine with a temperature profile of 210/200/190/180/170°C. The test specimens' dimensions corresponded to those specified in ASTM D638 (tensile test) and ASTM D256 (impact test). The sample formulations and codes are summarized in Table 1.

Table 1. Compositions of Samples

Sample	Composition (wt%)		
	PP	PP-g-MA	Organophilic clay
PP	100	-	-
PP/clay 97/3 (Exp.1)	97	-	3
PP/PPMA/clay 95/5/3 (Exp.2)	92	5	3
PP/PPMA 95/5 (Exp.3)	95	5	-

2.4. Characterization of Clays and Nanocomposites

The infrared analysis was performed on the clay samples using a Varian Excalibur 3100 spectrometer. The spectra were obtained in the 4000 to 400 cm^{-1} range, with samples pressed as KBr pellets.

The chemical composition of the clays was determined by X-ray fluorescence (XRF) in a WDX fluorescence spectrometer, Axios model (Panalytical). The semi quantitative results were calculated as oxides and normalized to 100%. The loss on ignition (LOI) was determined according to $\text{LOI} = (W_d - W_f)/W_d \times 100$, where W_d is the weight of the dry sample at 110°C and W_f is the weight of the calcined sample at 1000°C during 3 hours.

XRD measurements of clays were performed on a sample in the form of powder with an Ultima IV X-ray diffractometer (Rigaku Corporation) using a potential difference of 40 kV and tube electric current of 20 mA. The scan was performed in the angular region 0.9 to 10° (2 θ) at 1° (2 θ)/min. The radiation used was $\text{CuK}\alpha$ with $\lambda = 1.5418 \text{ \AA}$. For analysis of nanocomposites, 0.2-mm thick films were compression molded by heating at 190°C under 69 MPa for 15 min, and cooling for 5 min in a cold press. The interplanar distance (d) was calculated based on the results, according to Bragg's law.

The thermal stability of the nanocomposites was evaluated by thermogravimetric analysis (TGA) in a TA Instruments model Q500 analyzer. The samples were heated from 30 up to 700°C, at a heating rate of 10°C/min under nitrogen flow.

The thermal behavior of the materials was analyzed in a TA Instruments Q1000 differential scanning calorimeter (DSC). The samples were heated to 200°C, kept at this temperature for 5 min, and then cooled to room temperature at 10°C/min. They were then reheated to 200°C at same heating rate. The crystallization and melting thermograms were recorded from the cooling and second heating cycles, respectively. The melting temperature (T_m) and crystallization temperature (T_c) were determined from the DSC diagrams. Sample crystallinity content was calculated using a PP fusion enthalpy reference value of 190 J/g [28].

The clay dispersion of nanocomposite samples was examined by transmission electron microscopy (TEM). Ultra-thin sections (50 nm) were obtained with a Leica EM UC6 ultra-microtome and collected on a copper grid. TEM images were recorded with a FEI-Tecnaï G2 Spirit with a LaB₆ filament and acceleration voltage of 120 kV.

The tensile properties of PP and PP/PP-g-MA/clay nanocomposites were determined using a Shimadzu AG-I universal testing machine with a 5 kN load cell. Tests were conducted according to ASTM D 638 using Type I test specimen dimensions (seven specimens for each test). A crosshead speed of 20 mm/min was employed. The Izod impact strength of notched specimens was determined in a CEAST model 9050 impact machine according to ASTM D256.

3. Results and Discussion

3.1. Characterization of Clays

3.1.1. X-ray Fluorescence (XRF)

Table 2 presents the results of chemical analysis obtained by X-ray fluorescence (XRF) for the pristine clay (JG), the homoionic clay (JG-Na), and the organically modified clay (JG-Org), prepared with cetyltrimethyl ammonium chloride.

Table 2. Chemical Composition of Pristine, Homoionic and Organophilic Bentonites

Oxides	JG (%)	JG-Na(%)	JG-Org (%)
SiO ₂	46.2	47.0	38.8
Al ₂ O ₃	27.2	27.4	23.3
Na ₂ O	0.28	2.5	0.10
MgO	1.5	1.1	0.89
K ₂ O	0.29	0.30	0.24
CaO	1.21	0.85	0.35
TiO ₂	0.88	0.98	0.80
Fe ₂ O ₃	3.42	4.18	3.07
Cl	0.05	0.63	0.82
LOI (1000°C)	18.86	14.89	31.53

LOI – Weight loss on ignition

The JG clay is a polycationic clay that has different exchangeable cations in the interlayer (Table 2), which makes this clay an inhomogeneous material. In order to obtain a more homogeneous interlayer spacing, an exchange of existing cations by a single type of ion, Na⁺, was performed. The results in Table 2 indicate that this clay was modified. The MgO and CaO content in the JG-Na clay showed a significant decline compared to those presented by the JG clay. Furthermore, there was a significant increase in the Na₂O content after homoionization of the JG clay, which confirms the above results.

Regarding the clay modified with the quaternary ammonium salt (JG-Org), the oxide concentration in this clay, especially of the calcium and sodium oxides, showed

a significant reduction compared to the oxide content in the JG-Na clay. This result indicates an intercalation of cetyltrimethyl ammonium chloride in the interlayer space of the clay. The low Na₂O content in the JG-Org clay, 0.10% (wt/wt), is evidence of a high yield in the exchange of Na⁺ ions with NH₃R⁺ ions.

Another factor which can be used to confirm the organophilization process of clay is the weight loss on ignition (LOI) (Table 2), which is the loss of intercalated water together with loss of water of hydroxyls of clay minerals, organic matter and carbonates [19]. For the samples studied, the LOI presented values of 18.86% for the unmodified clay (JG) and 31.53% for the organically modified clay (JG-Org). The highest LOI value presented by JG-Org indicates that the quaternary ammonium salt was incorporated into this clay structure, leading to an organoclay. Similar results were obtained by Barbosa *et al.* [29] investigating organophilization of bentonite clay with different quaternary ammonium salts.

3.1.2. Fourier-Transform Infrared Spectroscopy (FTIR)

Figure 1 shows the FTIR spectra of JG, the homoionic (JG-Na), and organically modified (JG-Org) clays.

All the samples showed absorption bands at 3698 and 3623 cm⁻¹, attributed to the OH stretching, corresponding to structural hydroxyl groups of the clay. Absorption bands at 3400 and 1638 cm⁻¹, attributed to the angular vibration of the OH group and related to the adsorbed water and the hydration water present in the clay, can also be seen in the spectra [30].

Characteristic absorption of montmorillonite clay can be observed in the region between 1115 and 1034 cm⁻¹, related to the Si-O bond, and at 915, 798 and 542 cm⁻¹, corresponding to the octahedral layers of the aluminosilicate. No changes were found in the spectrum of sodium clay (JG-Na) (b) in relation to the pristine clay (JG) (a).

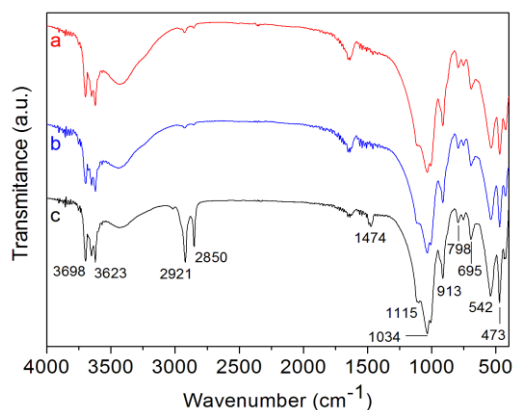


Figure 1. FTIR spectra of the bentonite clays: (a) JG, (b) JG-Na and (c) JG-Org

The organoclay presented new characteristic absorption bands at 2921 cm⁻¹, corresponding to asymmetrical stretching of the C-H bond (CH₃ and CH₂ groups); at 2850 cm⁻¹, attributed to the symmetrical stretching of the

C-H bond (CH₃ and CH₂ groups), and at 1474 cm⁻¹, corresponding to angular deformations of the C-H bond (CH₃ and CH₂ groups). Several studies in the literature [3,11,20,31] have shown the presence of these main absorption bands in the infrared region in different clays modified with quaternary ammonium salts. These findings indicate that ammonium cations were intercalated between the clay galleries.

3.1.3. X-ray Diffraction (XRD)

Analyses by X-ray diffraction (XRD) were conducted in order to verify the possible intercalation of quaternary ammonium salt between the lamellae of JG clay. Figure 2 shows the diffractograms.

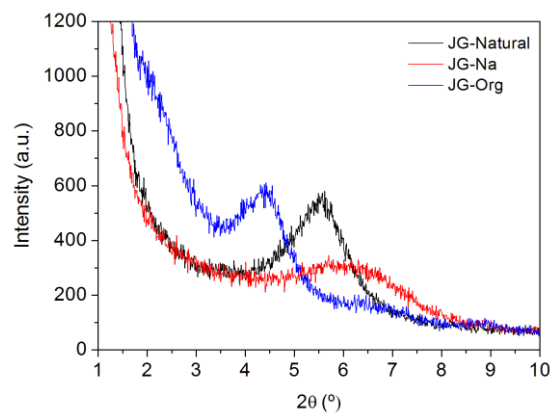


Figure 2. Diffractograms of the bentonite clays

The diffractogram of JG clay shows the characteristic peak of bentonite clays at $2\theta = 5.57^\circ$. The diffractograms of the modified clays (JG-Na and JG-Org) show that there were changes in the displacement of the peak characteristic diffraction of JG clay with the two treatments used in the cation exchange process. Table 3 shows the values of the characteristic diffraction peaks of JG, JG-Na and JG-Org and the corresponding basal plane spacings (d_{001}).

Table 3. Values of Diffraction Peaks (2θ) and Basal Plane Spacings (d_{001}) of Pristine, Homoionic and Organophilic Bentonites

Clays	2θ (°)	d_{001} (Å)
JG	5.57	15.88
JG-Na	6.15	14.39
JG-Org	4.42	20.00

The XRD results of JG-Na show that the basal plane spacings of this clay decreased from 15.88 to 14.39 Å, attributed to the exchange of the cations in this clay with sodium ions. Replacement of exchangeable cations of bentonite clays by Na⁺ ions allows obtaining clays with more homogeneous interlayer spacing, which makes the organophilization of these clays easier. The organoclay shows a peak at 4.42°, corresponding to a d_{001} spacing of 20.00 Å. According to the results obtained, the d_{001} spacing increased from 15.88 Å in the neat bentonite (JG) to 20.00 Å in the organophilized bentonite. The significant increase

in d_{001} of this organoclay indicates there was effective quaternary ammonium cation intercalation in the layers.

3.2. Characterization of Nanocomposites

3.2.1. Structure and Morphology

The structure and morphology of the nanocomposites were evaluated by X-ray diffraction and transmission electron microscopy, respectively. X-ray diffraction patterns of the PP/clay and PP/PP-g-MA/clay nanocomposites as well as the organoclay (used as reference), in the region corresponding to 2θ values from 1° to 10° are presented in Figure 3.

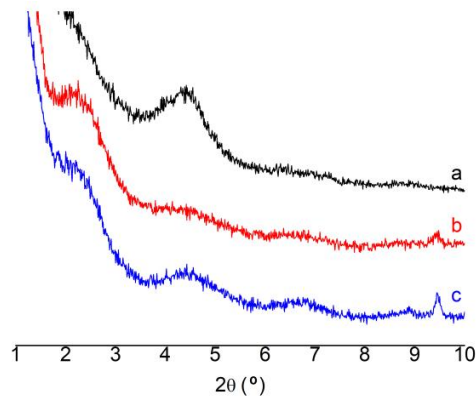


Figure 3. XRD patterns of the organoclay (a), PP/clay (b) and PP/PPMA/clay (c)

The values of the characteristic diffraction peaks of the samples and their respective interplanar distances (d) are reported in Table 4.

Table 4. Values of Diffraction Peaks (2θ) and Interplanar Distances (d) of Organoclay, PP/clay and PP/PP-g-MA/clay Nanocomposites

Samples	2θ ($^\circ$)	d (\AA)
Organoclay	4.42	20.00
PP/clay	2.24	39.40
	4.50	19.61
	6.77	13.04
PP/PPMA/clay	2.49	35.44
	4.44	19.88
	6.65	13.28

The organoclay sample presents a characteristic diffraction peak, 4.42° , and a d_{001} spacing of 20.00 \AA . The basal plane spacing of PP/clay sample is 39.40 \AA . This increase in the d_{001} spacing may be attributed to the partial intercalation of PP molecular chains into the interlayer space of the organoclay. A second broad peak, related to a distance of 19.61 \AA ($2\theta = 4.50^\circ$), which is close to the distance of 20.00 \AA of the clay modified with quaternary ammonium salt, can be attributed to the small part of the montmorillonite layers that were not intercalated by PP molecules. A third broad diffraction peak, corresponding to an interlayer spacing of 13.04 \AA ($2\theta = 6.77^\circ$), might be due to incomplete ion exchange and some residual MMT. Similar results

were observed by Araújo and co-authors (2007) in the characterization by X-ray diffraction of nanocomposites containing polyethylene (PE) and organically modified montmorillonite clay (OMMT) obtained via direct melt intercalation [32].

The X-ray diffraction patterns of the nanocomposite of PP with 3 wt% of organoclay and 5 wt% of PP-g-MA compatibilizer show a characteristic diffraction peak, 2.49° , and a d_{001} spacing of 35.44 \AA . This increase of d_{001} spacing can be attributed to intercalation of the polymer chains between the layers of the organoclay. A second broad peak is observed around $2\theta = 4.44^\circ$, assigned to an interlayer spacing of 19.88 \AA . The XRD pattern of this sample also shows a third broad diffraction peak related to an interlayer spacing of 13.28 \AA .

The PP/clay nanocomposites with or without the compatibilizer agent (PP-g-MA) experienced an increase in the interlayer distance with respect to the organoclay alone. Pérez and co-authors (2010) did not observe differences in interlayer spacing in PP/clay nanocomposites obtained in twin-screw co-rotating extruders with or without compatibilizer agent (PP-g-MA). This behavior was attributed to low concentration of the compatibilizer used to prepare the nanocomposites [33]. The results of XRD suggest that the PP/clay and PP/PP-g-MA/clay nanocomposites are partially intercalated.

In a recent paper [34] evaluated the interfacial properties of PE/clay/silver composites with different types of compatibilizers or adhesion promoters. The purpose of the work was to explore the ability of functional and maleated PE compatibilizers to exfoliate and disperse clay and silver nanoparticles and examine the effect on antimicrobial properties of hybrid PE/clay/silver nanocomposites. The XRD results obtained for nanocomposites with 10 and 20 wt% of PE-g-MA showed a noticeable diffraction peak that was shifted to lower angles and higher intergallery d_{001} spacing compared with the diffraction peak of the pure nanoclay. According to the authors, this indicates a certain degree of intercalation-exfoliation of the clay in the polymer matrix.

Sánchez-Valdez *et al.* (2010) evaluated the effect of various compatibilizers on the degree of exfoliation and optical properties of PE-clay nanocomposites in order to obtain nanocomposite films for greenhouse cover applications. XRD results showed that the addition of PEgMA increased the d_{001} spacing from 2.40 nm in the organoclay to 2.87 in the PE/PEgMA/clay nanocomposite, suggesting a better degree of intercalation for this compatibilizer [35].

Transmission electron microscopy (TEM) is the most efficient method available to describe the nanoscale dispersion of the clay in the polymer.

In this work, TEM micrographs were acquired to delineate the dispersion status of the organically modified clay in the PP matrix. Figure 4 shows the TEM micrographs of PP/clay and PP/PP-g-MA/clay nanocomposites. The dark regions correspond to the stacked clay particles. The clearer

regions correspond to the polymer intercalated between the clay platelets. The individual clay layers resulting of the delamination process of the clay particles correspond to the exfoliated structure of the clay lamellae [1,3,36,37]. All these morphologies are present in all micrographs. However, in the PP/PP-g-MA/clay nanocomposites, the partially exfoliated nanocomposites are slightly oriented in the injection direction. These results associated with the XRD data show that both partial intercalation and partial exfoliation nanocomposites morphologies were obtained.

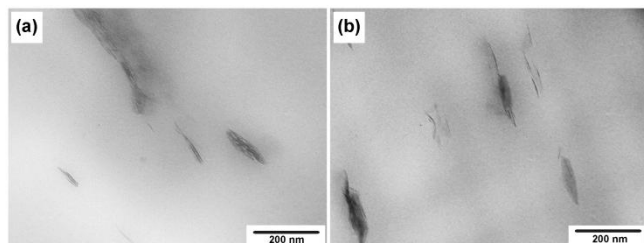


Figure 4. TEM micrographs of PP/clay (a) and PP/PPMA/clay (b)

3.2.2. Differential Scanning Calorimetry (DSC)

To evaluate the thermal properties of the nanocomposites, non-isothermal crystallization DSC scans were carried out. Table 5 shows values for melting temperature (T_m), crystallization temperature (T_c), melting enthalpy (ΔH_m) and crystallinity degree of PP, PP/clay, PP/PPMA/clay and PP/PPMA samples.

Table 5. Thermal Properties of PP, PP/Clay, PP/PPMA/clay and PP/PPMA Samples

Sample	T_c (°C)	T_m (°C)	ΔH_m (J/g)	Crystallinity degree (%)
PP	117.6	163.9	105.7	55.6
Exp.1	117.8	164.7	107.9	56.8
Exp.2	120.8	163.7	110.2	58.0
Exp.3	120.5	165.2	107.3	56.5

Table 5 shows that the melting temperature of PP/clay nanocomposites is very similar to that of polypropylene, indicating that there was no increase in the imperfection of the crystals due the clay layers. However, the crystallinity degree shows a slight increase, probably due to the nucleating effect of the PP-g-MA. The addition of PP-g-MA and clay to the polymer tends to increase its melting temperature. A greater number of DSC analysis is needed in order to obtain more conclusive results. Similar behavior was observed by Zaman and co-authors in evaluating thermal properties of polypropylene/organoclay nanocomposites with different compatibilizers prepared by melt compounding [40].

Table 5 shows that the PP crystallization temperature (T_c) was not affected by the addition of organoclay. However, with the addition of PP-g-MA compatibilizer, the crystallization peak is displaced to higher temperatures in relation to neat PP. This effect can be better visualized in Figure 5.

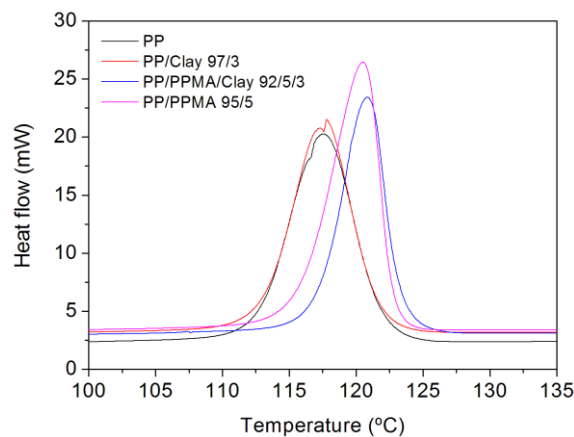


Figure 5. Crystallization peaks of PP, PP/clay, PP/PPMA/clay and PP/PPMA samples

The samples' crystallization behavior indicates that PP-g-MA acts as a nucleating agent for PP. Lai, Chen and Zhu (2009), in an evaluation of the effect of adding compatibilizers on the properties of PP/clay nanocomposites, also found a similar result in the crystallization behaviour of the PP/PP-g-MA/clay system. These authors noted an increase in the crystallization temperature for the PP/PP-g-MA and PP/POE-g-MA blends, indicating that the compatibilizers act as nucleating agents [39]. However, results obtained by other researchers have shown that the PP-g-MA does not cause significant change in the PP crystallization behavior [7].

Table 5 indicates that the PP/PPMA/clay nanocomposite presented the highest values of melting enthalpy (ΔH_m) and crystallinity. These results suggest that PP-g-MA acts effectively as a compatibilizer for the PP/clay system, improving the interaction between the hydrophilic surface of clay and the hydrophobic polypropylene as well as the clay distribution in the PP matrix.

3.2.3. Thermogravimetric Analysis (TGA)

Determination of the thermal properties and stability of polymer clay nanocomposites is very important, mainly due to possible variations in the structure and degradation of the material from the processing conditions employed. At processing temperatures higher than the thermal stability of the organic salts used for modification of the clays, decomposition will take place [40]. In the present work, the processing temperatures were defined according to evaluation of the thermal stability of organically modified clay and processing conditions observed in the literature [41]. The thermogravimetric analyses were used to investigate the thermal stability of the PP/clay and PP/PPMA/clay nanocomposites. With this purpose, the degradation onset temperature (T_{onset}) was determined. The results obtained are reported in Table 6.

Table 6 shows that the thermal stability of polypropylene was not improved by the addition of clay. However, the addition of PP-g-MA to PP/clay nanocomposite increased the thermal stability of this nanocomposite. This result

combined with those presented in Table 5 indicates that the PP/PPMA/clay 92/5/3 nanocomposite presents superior thermal properties. The TGA curves also can be seen in Figure 6.

Table 6. T_{onset} of PP, PP/clay and PP/PPMA/clay Nanocomposites

Sample	T_{onset} (°C)
PP	429
PP/clay 97/3 (Exp.1)	429
PP/PPMA/clay 92/5/3 (Exp.2)	434

Generally, the PP/clay nanocomposites present an increase of the initial degradation temperature (T_{onset}) compared to the neat polymer. This result can be attributed to two effects: the restricted mobility of the polymeric chains caused by the clay particles and the formation of a heat barrier created by the migration of clay particles to the surface, hindering the release of gases from the degradation of nanocomposites [40].

Perez *et al.* (2010) in a study of PP/clay nanocomposites, observed that the thermal behavior of these materials depends on the polypropylene melt flow rate (MFR). These researchers found no changes in thermal stability of the PP (MFR = 2 g/10 min)/clay nanocomposite compared to the PP. This effect, also observed for the PP/PPMA/clay, was attributed to the low MFR of the polypropylene, which makes incorporation of the polymer into the clay layers more difficult [33].

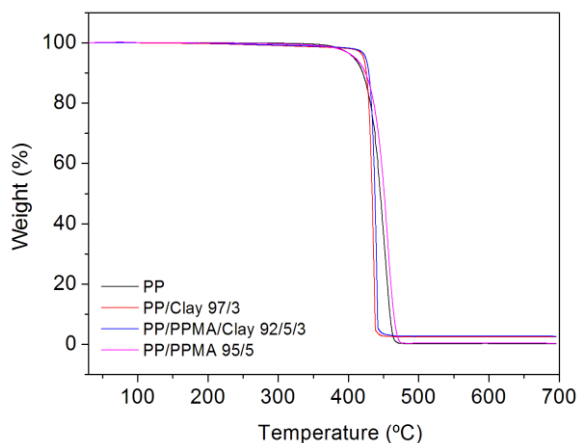


Figure 6. Weight loss of PP/PPMA/clay nanocomposites as a function of temperature

The higher thermal stability of PP/PPMA/clay verified in this work can be explained by the lower mobility of the polymer chains due to the anchoring effect of the PP-g-MA, improving the interaction between the clay and the polymeric chains. The results obtained also suggest there was no increase of the PP thermal stability with the clay addition due to the partial intercalation of the polypropylene into clay platelets.

3.2.4. Tensile Properties

The study of the mechanical properties of nanocomposites

is very complex, since these properties are influenced by several variables, such as processing machinery [3,42]; processing conditions [42]; chemical nature of the clay surface modifier [42]; type and concentration of clay and compatibilizer [42-44]; compatibilizer/nanoclay ratio [44]; viscosity of the compatibilizer, and polypropylene melt flow rate (MFR) [33]. Therefore, several studies have been published showing a large improvement of the mechanical properties of PP/clay nanocomposites, while others have shown no noteworthy changes in the mechanical behavior of this polymer [3]. Table 7 presents the mechanical property data obtained in this work.

Table 7. Tensile Properties of PP, PP/clay and PP/PPMA/clay Nanocomposites

Sample	Young's Modulus (MPa)	Tensile Strength (MPa)	Elongation at Break (%)
PP	1384 ± 20	35.26 ± 0.35	13 ± 4
Exp.1	1370 ± 10	35.46 ± 0.18	37 ± 2
Exp.2	1377 ± 13	36.37 ± 0.21	102 ± 12

Table 7 shows there was no improvement in Young's modulus of polypropylene with the addition of clay. Similar results have been obtained by other researchers [3,33,41,45]. According to Rodrigues *et al.* (2007) in a study of the mechanical properties of polypropylene/Brazilian bentonite clay nanocomposites, the addition of increasing amounts of clay as well the type of compatibilizer and the clay organophilization process had no effect on the polypropylene tensile modulus [3]. These researchers reported that significant improvements of PP tensile modulus in PP/clay nanocomposites obtained by other authors were attributed to good interaction between the polymer and clay surface, resulting in better intercalation of this polymer between the clay platelets.

Morales *et al.* (2012) evaluated the mechanical properties of systems based on polypropylene (PP) and commercial organophilic montmorillonite, prepared by melt intercalation. The nanocomposites obtained presented mechanical properties comparable to those presented by composites filled with micron-sized mineral particles. This result was attributed to the unsatisfactory dispersion of clay that occurred despite the partial intercalation and exfoliation of this filler [7].

The tensile strength of PP/PPMA/clay nanocomposite (Table 7) showed a slight increase compared to those presented by both neat PP and PP/clay nanocomposite, due to the better dispersion of the clay promoted by the compatibilizer's addition. The finer morphology should contribute to increase the matrix resistance. However, there are indications that improvement in tensile strength of PP/clay nanocomposites is very small at low clay concentrations (below 10%) [46].

Arunachalam *et al.* (2015) prepared polypropylene clay nanocomposites (PP-CNs) by melt compounding with different nanoclays and at varying compatibilizer/nanoclay ratios. For the PP-CNs prepared with the nanoclay Bentone

38 (OMHT), the authors observed that when the compatibilizer content increased, there was an increase in yield stress. According to the authors, this confirms that the interaction of OMHT clay layers and the polymer matrix is high when the compatibilizer content increases [40].

Table 7 shows that both nanocomposites (PP/clay and PP/PMMA/clay) presented higher elongation at break than polypropylene and that this increase was more pronounced when the compatibilizer was added to PP/clay nanocomposite. Similar results were obtained by Rodrigues *et al.* (2007). They found that the addition of clay to polypropylene in all systems studied led to an increase of the elongation at break. This result was explained by the tactoids' delamination during tensile deformation after the yield point [3]. The increase of the elongation at break obtained in this work may also be due to a possible plasticizing effect of the compatibilizer on the polypropylene chains. Table 8 indicates a significant increase of PP toughness due to the formation of the PP/clay nanocomposites, especially in the presence of the PP-g-MA compatibilizer.

Table 8. Toughness of PP, PP/clay and PP/PMMA/clay Nanocomposites

Sample	Tenacity (MJ/m ³)
PP	9 ± 3
PP/Clay 97/3 (Exp.1)	18 ± 1
PP/PMMA/Clay (Exp.2)	35 ± 3

3.2.5. Impact Strength

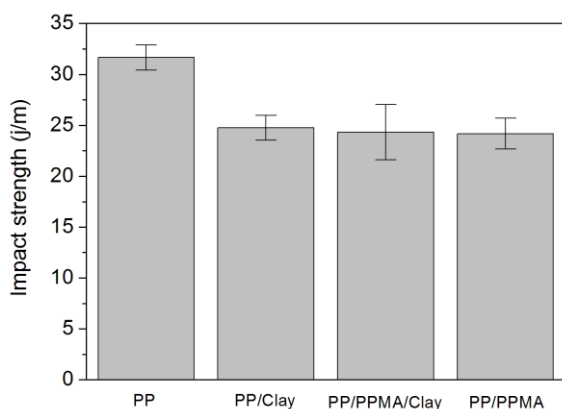


Figure 7. Izod impact strength of PP, PP/clay and PP/PMMA/clay nanocomposites

The Figure 7 shows the Izod impact strength of polypropylene and the PP/clay nanocomposites. The results show that the addition of clay as well as the addition of clay and compatibilizer together decreased the impact strength of polypropylene. This result can be attributed to the partial dispersion of the clay in the PP matrix. It is not easy to predict the effect of nanosize particles on the impact strength of nanocomposites. Some researchers have reported that impact strength is strongly influenced by the content of coupling agent and also by the quality of the clay [41]. According to Chen *et al.* (2009), it is difficult to predict how nano-reinforcements will affect impact strength, because of

the confounding effects of crystallinity, spherulite size, preferred orientation or processing variables [46].

4. Conclusions

The results obtained in this work indicate there was partial intercalation of polypropylene chains in the clays layers. The PP/PMMA/clay nanocomposite presented higher thermal stability and crystallization temperature than the PP matrix. The Young's modulus and tensile strength of PP were not affected. However, there was a significant increase in the elongation at break. The impact strength decreased slightly with the addition of clay and compatibilizer. These findings show that Brazilian bentonite clay can be used as a filler in PP/nanocomposites. However, other experimental conditions should be evaluated to obtain better dispersion of clay in the polymer matrix and a larger improvement in the properties.

ACKNOWLEDGEMENTS

This study was financed in part by the Coordenação de Aperfeiçoamento de Pessoal de Nível Superior - Brasil (CAPES) - Finance Code 001. We also thank Conselho Nacional para o Desenvolvimento Científico e Tecnológico (CNPq) and Fundação de Amparo à Pesquisa do Estado do Rio de Janeiro (FAPERJ) for financial support and Centro de Tecnologia Mineral (CETEM) for supplying the clay samples.

REFERENCES

- [1] A. I. Alateyah, H. N. Dhakal, Z. Y. Zhang. "Processing, properties and applications of polymer nanocomposites based on layer silicates: A review", *Advances in Polymer Technology*, vol. 32, pp. 21368(1-36), 2013.
- [2] F. C. Morelli, A. Ruvolo Filho. "Nanocompósitos de polipropileno e argila organofílica: difração de raios X, espectroscopia de absorção na região do infravermelho", *Polímeros*, vol. 20, pp. 121-125, 2010.
- [3] A. W. Rodrigues, M. I. Brasileiro, W. D. Araújo, E. M. Araújo, G. N. Neves, T. J. A. Melo. "Desenvolvimento de nanocompósitos polipropileno/argila bentonita brasileira: I tratamento de argila e influência de compatibilizantes nas propriedades mecânicas", *Polímeros: Ciência e Tecnologia*, vol. 17, pp. 219-227, 2007.
- [4] M. Alexandre, P. Dubois. "Polymer-layered silicate nanocomposites: preparation, properties and uses of a new class of materials", *Materials Science and Engineering*, vol. 28, pp. 1-63, 2000.
- [5] L. B. Paiva, A. R. Morales, T. R. Guimarães. "Propriedades mecânicas de nanocompósitos de PP e montmorilonita organofílica", *Polímeros: Ciência e Tecnologia*, vol. 16, pp. 136-140, 2006.

- [6] R. A. Paz, A. M. D. Leite, E. M. Araújo, T. J. A. Melo, R. Barbosa, E. N. Ito. "Nanocompósitos de poliamida 6/argila organofílica", *Polímeros: Ciência e Tecnologia*, vol. 18, pp. 341-347, 2008.
- [7] A. R. Morales, L. B. Paiva, D. Zattarelli, T. R. Guimarães. "Morphology structure and mechanical properties of polypropylene modified with organophilic montmorillonite", *Polímeros*, vol. 22, pp. 54-60, 2012.
- [8] T. T. Zhu, C. H. Zhou, F. B. Kabwe, Q. Q. Wu, C. S. Li, J. R. Zhang. "Exfoliation of montmorillonite and related properties of clay/polymer nanocomposites", *Applied Clay Science*, vol. 169, pp. 48-66, 2019.
- [9] M. Weltrowski, P. I. Dolez. "Compatibilizer polarity parameters as tools for predicting organoclay dispersion in polyolefin nanocomposites", *Journal of Nanotechnology*, vol. 2019, pp. 1-9, 2019.
- [10] K. Sung, S. Nakagawa, C. Kim, N. Yoshie. "Fabrication of nacre-like polymer/clay nanocomposites with water-resistant and self-adhesion properties", *Journal of Colloid and Interface Science*, vol. 564, pp. 113-123, 2020.
- [11] E. V. D. G. Líbano, L. L. Y. Visconte, E. B. A. V. Pacheco. "Propriedades térmicas de compósitos de polipropileno e bentonita organofílica", *Polímeros*, vol. 22, pp. 430-435, 2012.
- [12] A. R. V. Silva, H. C. Ferreira. "Argilas bentoníticas: conceitos, estruturas, propriedades, usos industriais, reservas, produção e produtos/fornecedores nacionais e internacionais", *Revista Eletrônica de Materiais e Processos*, vol. 3, pp. 26-35, 2008.
- [13] R. R. Menezes, P. M. Souto, L. N. L. Santana, G. A. Neves, R. H. G. A. Kiminami, H. C. Ferreira. "Argilas bentoníticas de Cubati, Paraíba, Brasil: Caracterização física-mineralógica", *Cerâmica*, vol. 55, pp. 163-169, 2009.
- [14] E. M. Araújo, and T. J. A. Melo, *Nanocompósitos poliméricos – Pesquisas na UFCG com argilas bentoníticas*, 1st ed., Campina Grande, Brazil, EDUFCEG, 2012.
- [15] C. I. R. de Oliveira, M. C. G. Rocha, A. L. N. da Silva, L. C. Bertolino. "Characterization of bentonite clays from Cubati, Paraíba (Northeast of Brazil)", *Cerâmica*, vol. 62, pp. 272-277, 2016.
- [16] I. D. S. Pereira, "Estudos de novas jazidas de argilas bentoníticas do estado da Paraíba, visando seu uso em fluidos de perfuração de poços de petróleo" Masters Dissertation, Universidade Federal de Campina Grande, Campina Grande, Brazil, Aug. 2014.
- [17] E. V. D. Gomes, L. L. Y. Visconte, E. B. A. V. Pacheco. "Processo de organofiliação de vermiculita brasileira com cloreto de cetiltrimetilamônio", *Cerâmica*, vol. 56, pp. 44-48, 2010.
- [18] R. Barbosa, E. M. Araújo, T. J. A. Melo, E. N. Ito. "Comparison of flammability behavior of polyethylene/Brazilian clay nanocomposites and polyethylene/flame retardants", *Materials Letters*, vol. 61, pp. 2575-2578, 2007.
- [19] P. Souza Santos. *Ciência e Tecnologia de Argilas*, 1st ed., São Paulo, Brazil, Edgar Blücher, 1992.
- [20] L. B. Paiva, A. R. Morales, F. R. V. Diaz. "Argilas organofílicas: características, metodologias de preparação, compostos de intercalação e técnicas de caracterização", *Cerâmica*, vol. 54, pp. 213-226, 2008.
- [21] L. B. Paiva, A. R. Morales, F. R. V. Diaz. "Organoclay: properties, preparation and applications", *Applied Clay Science*, vol. 42, pp. 8-24, 2008.
- [22] S. K. Sharma, S. K. Nayak. "Surface modified clay/polypropylene (PP) nanocomposites: Effect on physic-mechanical, thermal and morphological properties", *Polymer Degradation and Stability*, vol. 94, pp. 132-138, 2009.
- [23] K. S. Santos, R. Demori, R. S. Mauler, S. A. Liberman, M. A. S. Oviedo. "The influence of screw configuration and feed mode on the dispersion of organoclay on PP", *Polímeros*, vol. 23, pp. 175-181, 2013.
- [24] P. Liborio, V. A. Oliveira, M. F. V. Marques. "New chemical treatment of bentonite for the preparation of polypropylene nanocomposites by melt intercalation", *Applied Clay Science*, vol. 111, pp. 44-49, 2015.
- [25] W. S. Cavalcanti, G. F. B. Brito, P. Agrawal, T. J. A. Melo, G. A. Neves, M. M. Dantas. "Purificação e organofiliação em escala piloto de argilas bentoníticas com tensoativo não iônico e aplicação em nanocompósitos poliméricos", *Polímeros*, vol. 24, pp. 491-500, 2014.
- [26] M.L López-Quintanilla, S. Sánchez-Valdés, L.F. Ramos de Valle, R. Guedea Miranda, "Preparation and mechanical properties of PP/PP-g-MA/Org-MMT nanocomposites with different MA content", *Polymer Bulletin*, vol. 57, pp. 385-393, 2006.
- [27] C. K. Hong, M. J. Kim, S. H. Oh, Y. S. Lee, C. Nah. "Effects of polypropylene-g-(maleic anhydride/styrene) compatibilizer on mechanical and rheological properties of polypropylene/clay nanocomposites", *Journal of Industrial and Engineering Chemistry*, vol. 14, pp. 236-242, 2008.
- [28] F. O. M. S. Abreu, M. M. C. Forte, S. A. Liberman. "SBS and SEBS block copolymers as impact modifiers for polypropylene compounds", *Journal of Applied Polymer Science*, vol. 95, pp. 254-263, 2005.
- [29] R. Barbosa, E. M. Araújo, A. D. Oliveira, T. J. A. Melo. "Efeito de sais quaternários de amônio na organofiliação de uma argila bentonita nacional", *Cerâmica*, vol. 52, pp. 264-268, 2006.
- [30] I. F. Leite, C. M. Raposo, S. M. L. Silva. "Caracterização estrutural de argilas bentoníticas nacional e importada: antes e após o processo de organofiliação para utilização como nanocargas", *Cerâmica*, vol. 54, pp. 303-308, 2008.
- [31] R. R. Menezes, M. M. Ávilla Júnior, L. N. L. Santana, G. A. Neves, H. C. Ferreira. "Comportamento de expansão de argilas bentoníticas organofílicas do estado da Paraíba", *Cerâmica*, vol. 54, pp. 152-159, 2008.
- [32] E. M. Araújo, R. Barbosa, A. W. B. Rodrigues, T. J. A. Melo, E. N. Ito. "Processing and characterization of polyethylene/Brazilian clay nanocomposites", *Materials Science and Engineering A*, vol. 445-446, pp. 141-147, 2007.
- [33] M. A. Pérez, B. L. Rivas, S. M. Rodrigues, A. Maldonato, C. Venegas. "Polypropylene/clay nanocomposites: synthesis and characterization", *Journal of the Chilean Chemical Society*, vol. 55, pp. 440-444, 2010.

- [34] M. C. Ibarra-Alonso, S. Sánchez-Valdes, E. Ramírez-Vargas, S. Fernandez-Tavizón, J. Romero-Garcia, A. S. Ledezma-Perez, L. F. Ramos de Valle, O. S. Rodrigues-Fernandez, A. B. Espinosa-Martinez, J. G. Martinez-Colunga, E. M. Cabrera-Álvarez. "Preparation and characterization of polyethylene/clay/silver nanocomposites using functionalized polyethylenes as an adhesion promoter", *Journal of Adhesion Science and Technology*, vol. 29, pp. 1911-1923, 2015.
- [35] S. Sánchez-Valdez, J. Méndez-Nonell, F. J. Medellín-Rodríguez, E. Ramírez-Vargas, J. G. Martínez-Colunga, L. F. R. De Valle, M. Monfragón-Chaparro, M. L. López-Quintanilha, M. L. García-Salazar. "Evaluation of different amine-functionalized polyethylenes as compatibilizers for polyethylene film nanocomposites", *Polymer International*, vol. 59, pp. 704-711, 2010.
- [36] L. B. Paiva, A. R. Morales, M. C. Branciforti, R. E. S. Bretas. "Organophilic bentonites based on Argentinean and Brazilian bentonites. Part 2: Potential evaluation to obtain nanocomposites". *Brazilian Journal of Chemical Engineering*, vol. 29, pp. 751-762, 2012.
- [37] V. Mittal. "Polymer Layered Silicate Nanocomposites: A Review", *Materials*, vol.2, pp. 992-1057; 2009.
- [38] H. U. Zaman, P. D. Hun, R. A. Khan, K. B. Yoon. "Polypropylene/clay nanocomposites: effect of compatibilizer on the morphology, mechanical properties and crystallization behaviors", *Journal of Thermoplastic Composite Materials*, vol. 27, pp. 338-349, 2014.
- [39] S. M. Lai, W. C. Chen, X. S. Zhu. "Melt mixed compatibilized polypropylene/clay nanocomposites: Part 1 – the effect of compatibilizers on optical transmittance and mechanical properties", *Composites Part A*, vol. 40, pp. 754-765, 2009.
- [40] S. Arunachalam, M. G. Battisti, C. T. Vijayakumar, W. Friesenbichler. "An investigation of mechanical and thermal properties of polypropylene clay nanocomposites containing different nanoclays", *Macromolecular Materials and Engineering*, vol. 300, pp. 966-976, 2015.
- [41] D. García-López, O. Picazo, J. C. Merino, J. M. Pastor. "Polypropylene-clay nanocomposites: effect of compatibilizing agents on clay dispersion", *European Polymer Journal*, vol. 39, pp. 945-950, 2003.
- [42] Q. T. Nguyen, D. G. Baird. "Preparation of polymer-clay nanocomposites and their properties", *Advances in Polymer Technology*, vol. 25, pp. 270-285, 2006.
- [43] S. H. Bahrami, Z. Mirzaie. "Polypropylene/modified nanoclay composite-processing and dyeability properties", *Word Applied Sciences Journal*, vol. 13, 493-501, 2011.
- [44] J. H. Park, H. M. Lee, I. J. Chin, H. J. Choia, H. K. Kim, W. G. Kang. "Intercalated polypropylene/clay nanocomposites and its physical characteristics", *Journal of Physics and Chemistry of Solids*, vol. 69, pp. 1375-1378, 2008.
- [45] S. S. Ray, M. Okamoto. "Polymer/layered silicate nanocomposites: a review from preparation to processing", *Progress in Polymer Science*, vol. 28, pp. 1539-1641, 2003.
- [46] B. Chen, J. R. G. Evans. "Impact strength of polymer-clay nanocomposites", *Soft Matter*, vol. 5, pp. 3572-3584, 2009.